Geoderma 464 (2025) 117641

Contents lists available at ScienceDirect

Geoderma

journal homepage: www.elsevier.com/locate/geoderma

Sustained use of DMPP reduces its mitigation potential for N_2O emissions: Field evidence and global implications

Zhutao Li [a], Roland Bol [b], Pinshang Xu [a], Zhaoqiang Han [a,c], Jie Wu [a,c], Xiang Gao [a], Shumin Guo [a], Xiaomeng Bo [a], Haiyan Lin [a], Mengxue Shen [a], Zhiwei Zhang [a], Zhe Xu [a], Jinyang Wang [a,c,*], Jianwen Zou [a,c,*]

[a] Key Laboratory of Low-carbon and Green Agriculture in Southeastern China, Ministry of Agriculture and Rural Affairs, College of Resources and Environmental Sciences, Nanjing Agricultural University, Nanjing 211800 Jiangsu, China
[b] Institute of Bio- and Geosciences: Agrosphere (IBG-3), Forschungszentrum Jülich 52425 Jülich, Germany
[c] Jiangsu Key Laboratory of Low Carbon Agriculture and GHGs Mitigation, Jiangsu Collaborative Innovation Center for Solid Organic Waste Resource Utilization, Nanjing 211800 Jiangsu, China

ARTICLE INFO

Handling Editor: Diego Abalos

Keywords:
N_2O
Nitrification inhibitor
DMPP
Ammonia oxidizers
Microbial adaptation
Global prediction
Sustainable nitrogen management

ABSTRACT

Nitrogen fertilization is a major driver of nitrous oxide (N_2O) emissions, and nitrification inhibitors such as 3,4-dimethylpyrazole phosphate (DMPP) are widely used to mitigate them. However, the long-term effectiveness of DMPP remains uncertain. Here, in a three-year field trial in acidic tea plantation soils under fertilized conditions, we demonstrate that the N_2O mitigation efficacy of DMPP progressively declines. This decline was mechanistically linked to treatment-induced microbial community adaptations: DMPP initially suppressed ammonia-oxidizing bacteria (AOB) but over time prompted a compensatory increase in ammonia-oxidizing archaea (AOA) and a compositional shift within the AOB community from *Nitrosospira* to *Nitrosomonas*. In our co-occurrence network analysis, the application of DMPP intensified niche competition and increased modularity, indicating enhanced microbial resilience. To contextualize these findings globally, we conducted a *meta*-analysis of 88 field studies, which confirmed that DMPP application reduced N_2O emissions by an average of 49 %, but its effectiveness declined significantly with prolonged use. Using a random forest model trained on global datasets, we predicted a 12 % reduction in mitigation potential after five years of consecutive DMPP application. These results demonstrate that sustained DMPP application under nitrogen-fertilized regimes triggers ecological feedbacks that diminish its practical benefits. We therefore conclude that adaptive management strategies, such as rotating different nitrification inhibitors, are imperative to counter microbial adaptation and sustain mitigation efforts in the long term.

1. Introduction

Nitrous oxide (N_2O) is a potent greenhouse gas, with atmospheric concentrations rising from pre-industrial levels of 270 ppb to 332 ppb in 2019, accelerating at an average rate of 0.85 ppb yr^{-1} since 1995. This increase is largely driven by anthropogenic activities (Canadell et al., 2021; Ravishankara et al., 2009). Emissions observed after 2010 have tracked the RCP 8.5 pathway predicted by the IPCC, thereby undermining international efforts to constrain global warming within 2 °C (Tian et al., 2020). Agriculture accounts for over half of anthropogenic N_2O emissions, primarily through nitrogen (N) fertilizer inputs that stimulate microbial N transformation processes (Bouwman et al., 2002). The biochemical complexity of N_2O production presents major challenges for mitigation, especially in intensive managed agroecosystems where excessive N inputs can overwhelm natural regulatory mechanisms. As global food demand increases, developing climate-smart strategies that decouple crop productivity from high N_2O emissions has become a critical goal.

Nitrification inhibitors (NIs) have been identified as an effective strategy for mitigating N_2O emissions by suppressing the microbial oxidation of ammonium. These compounds delay the transformation of ammonium (NH_4^+) to nitrate (NO_3^-), which in turn reduces the availability of NO_3^- for denitrification and thereby lowers N_2O production (Akiyama et al., 2025). Recent studies also suggest that NIs may

* Corresponding authorsat: Nanjing Agricultural University, Nanjing 211800, Jiangsu, China.
E-mail addresses: jywang@njau.edu.cn (J. Wang), jwzou21@njau.edu.cn (J. Zou).

https://doi.org/10.1016/j.geoderma.2025.117641
Received 5 August 2025; Received in revised form 25 November 2025; Accepted 28 November 2025
Available online 4 December 2025

influence denitrification by modulating the abundance or activity of N_2O reductase, which catalyzes the last step of N_2O reduction to dinitrogen (Friedl et al., 2020). Among commonly used NIs, such as 3,4-dimethylpyrazole phosphate (DMPP), dicyandiamide (DCD), and nitrapyrin, DMPP is notable for its strong adsorption to soil colloids, low volatility, and sustained efficacy at low application rates (Zerulla et al., 2001). While its short-term potential in reducing N_2O emissions is well documented, several multi-year studies report a gradual decline in DMPP efficacy (Abalos et al., 2017; Vilarrasa-nogué et al., 2020). Yet, the microbial mechanisms underlying this temporal attenuation remain poorly understood, and are often attributed to abiotic factors such as rainfall variability (Dong et al., 2021).

The effectiveness of DMPP, as a common NI and agricultural management tool, is shaped by complex interactions between agronomic practices, soil properties, and microbial communities. Soil N_2O emissions are governed by both proximal (e.g., soil pH, moisture, N availability) and distal (e.g., microbial composition, soil biogeography) regulators. Recent research suggest that microbial communities play a dominant role in determining the maximum N_2O emission potential, often outweighing the influence of the short-term abiotic variation (Xu et al., 2024). This raises the hypothesis that repeated applications of NIs may reshape nitrifier community structure and function, ultimately diminishing inhibitor effectiveness. This process parallels adaptive responses to other chemical pressures such as pesticides and antibiotics, where sustained selective pressure can lead to functional redundancy, niche partitioning, or resistance evolution in microbial communities (Andersson and Hughes, 2010; Kurenbach et al., 2015). For instance, ammonia-oxidizing bacteria (AOB) may shift towards DMPP-tolerance lineages, while ammonia-oxidizing archaea (AOA), which are less sensitive to DMPP, may compensate for suppressed AOB activity (Beeckman et al., 2018; Prosser and Nicol, 2012). Such microbial adaptations could reduce the long-term efficacy of DMPP and warrant deeper investigation into the ecological basis of N_2O mitigation outcomes.

The performance of DMPP is strongly modulated by interactions among soil properties, microbial communities, and climate. Moderate conditions (15–25 °C; 60–80 % water-filled pore space) favor its inhibitory action, while extreme heat (>30 °C) can accelerates DMPP degradation, particularly in subtropical or tropical systems (Nair et al., 2021). DMPP tends to persist longer in temperate zones. Soil texture further influences its effectiveness: clay-rich soils enhance retention, whereas sandy soils promote leaching and degradation. High soil organic matter may also stimulate microbial co-metabolism and reduce inhibitor persistence (Fisk et al., 2015; Lei et al., 2022). In addition, soil pH modulates AOA-AOB competition and nitrification rates, indirectly affecting DMPP efficiency (Fan et al., 2019; Prosser et al., 2020). These factors, together with geographic variability in soil biogeochemistry, create complex spatial and temporal patterns in NI performance. It remains unclear whether the efficacy of DMPP predictably declines with continued use across environmental gradients, and whether such trends can inform targeted inhibitor deployment strategies.

To address these knowledge gaps, we hypothesized that sustained DMPP application would alter the structure and function of nitrifier communities, inducing adaptive shifts that reduce its N_2O mitigation efficacy over time. We further hypothesized that this efficacy decline is governed by interactions among soil, climate, and microbial factors, and that these relationships can be modeled across diverse agroecosystems. To test these hypotheses, we performed a three-year field trial in a tea plantation characterized by high N input and elevated N_2O emissions (Wang et al., 2022), a representative high-emission system typically lacking long-term studies of NIs. We quantified changes in N_2O fluxes, soil biogeochemistry, and microbial community composition under DMPP treatment, with a focus on temporal trends in mitigation efficacy. We also conducted a global *meta*-analysis of 88 field studies to examine how environmental and management variables influence DMPP performance over time. By integrating multi-year field observations, global synthesis, and machine learning prediction, this study provides new cross-scale insights into the durability and agroecological context-dependence of nitrification inhibition strategies. These findings offer direct implications for adaptive N management and sustainable agricultural intensification.

2. Materials and methods

2.1. Site and experimental design

This trial represents a typical high-input tea cropping system, designed to evaluate the long-term effect of DMPP application on N dynamics and microbial communities when integrated with conventional fertilization. The experiment was conducted over three years (2020–2023) in a subtropical tea plantation in Jurong City, Jiangsu Province, China. The field featured a distinct banded fertilization pattern: fertilizers were applied exclusively to the inter-canopy zones (also referred to as rows in subsequent sampling descriptions), while the canopy zones directly beneath tea shrubs remained unfertilized to reflect local practice. This created two distinct sampling areas: the fertilized row/inter-canopy area and the unfertilized canopy area.

The experimental site comprised 20-year-old tea trees with an average canopy width of 1.2 m and an inter-canopy spacing of 0.4 m. The soil was classified as Planosol with an acidic pH of 4.2, a bulk density of 1.24 g cm^{-3}, soil organic carbon (SOC) content of 2.98 %, and total N content of 0.42 %. Three treatments were established using a randomized block design with three replicates and a plot size of 15 m^2 each. The treatments included: 1) Control (no fertilizer), 2) Conventional fertilization (F: 450 kg N ha^{-1} yr^{-1}, composed of 20 % cattle manure and 80 % urea), and 3) F + DMPP (applied at a rate of 1 % N-input). To maintain the nutrient balance, all treatments received 150 kg K_2O ha^{-1} and 150 kg P_2O_5 ha^{-1} annually. Fertilizers were band-applied exclusively in the inter-canopy zones, following local agricultural practices, with DMPP combined with urea during top-dressing. Gas and soil samples were separately collected from canopy and inter-canopy zones to capture spatial heterogeneity. Fertilization schedules and agronomic management details are summarized in Table S1. The fieldwork was interrupted during four COVID-19 lockdown periods: January-March 2021 (52 days), July-August 2021 (47 days), January-March 2022 (47 days) and March-May 2022 (65 days). In total, these lockdowns interrupted gas sampling for 211 days, accounting for approximately 19 % of the experimental period. It is important to note that the spring fertilization in March 2022 was completed normally, although subsequent gas sampling was suspended during the ensuing two-month lockdown. The cattle manure used as an organic amendment was alkaline (pH 8.07), with 2.96 % total N and a C/N ratio of 8.2. Meteorological conditions during the experimental period are shown in Fig. S1.

2.2. Gas sampling and flux measurements

The fluxes of N_2O were measured weekly and three times per week following fertilization using the static chamber-gas chromatography (GC) method (Zou et al., 2005). PVC collars (0.3 m diameter) were pre-installed 0.15 m into the soil under canopy and between-row areas two weeks before the first sampling. Gas samples (100 mL × 4) were collected at 10-minute intervals from chambers (0.6 m height) between 9:00–11:00 am. This 100 mL volume was determined to be optimal, being sufficient for representative GC analysis while avoiding significant negative pressure inside the chamber. All samples were immediately transferred and stored in pre-evacuated 100 mL aluminum foil gas bags, and analyzed within 24 h using a gas chromatograph (Agilent 7890A, USA). Fluxes were calculated using a non-linear curve fitting method as described by Kroon et al. (2008). Cumulative N_2O emissions (kg N ha^{-1}) from the entire plot (E) were calculated by weighting the measured cumulative emissions from the fertilized row area (E_{rows}) and the unfertilized canopy area (E_{canopy}) based on their respective areal proportions. The row and canopy zones accounted for 17 % and 83 % of the

total land area, respectively. Thus, the area-weighted cumulative emission was computed as follows:

$$E = 0.17 \times E_{rows} + 0.83 \times E_{canopy} \quad (1)$$

Direct N_2O emission factors (EFs, %) were estimated based on the default Tier 1 methodology recommended by the IPCC, following the approach outlined by Hergoualc'h et al. (2019):

$$EF = (E_N - E_0)/N_{-fer} \quad (2)$$

where E_N and E_0 refer to cumulative N_2O emissions (kg N ha^{-1}) from the fertilized and unfertilized plots, respectively, and N_{-fer} denotes the total N applied (kg N ha^{-1}).

The amount of N_2O emission reduction attributable to DMPP application (μg N m^{-2} h^{-1}) was quantified as the difference in N_2O flux between the DMPP-amended (F + DMPP) and the conventional fertilization (F) treatments, using the following equation:

$$DMPP\ effect = N_2O\ flux_{F+DMPP} - N_2O\ flux_F \quad (3)$$

2.3. Field sampling and soil property measurements

Soil temperature and moisture were recorded at a depth of 10 cm during each gas sampling event, using a handheld thermometer and MPM-160 sensor. Water-filled pore space (WFPS) was calculated by dividing the volumetric water content by the estimated total porosity, which was derived from the measured bulk density and an assumed particle density (2.65 g cm^{-3}).

For soil physicochemical analyses, composite soil samples (0–20 cm) were collected every two weeks from both the fertilized row and unfertilized canopy zones. These samples were sieved (2 mm) and stored at 4 °C for subsequent analysis.

To investigate the seasonal dynamics of N_2O production processes, functional gene abundance, and microbial community composition, additional soil samples were exclusively collected from the fertilized row zone at six key time points representing typical emission patterns after basal (winter) and top-dressing (summer) fertilization: 9 December 2020 (2020-Winter), 6 June 2021 (2021-Summer), 17 December 2021 (2021-Winter), 2 July 2022 (2022-Summer), 25 November 2022 (2022-Winter), and 14 June 2023 (2023-Summer). These samples were sieved and stored at −80 °C for molecular and process-based assays.

Gravimetric soil moisture was determined by drying fresh samples at 105 °C for 24 h. Bulk density was measured using undisturbed soil cores, while soil texture was analyzed following the hydrometer method described by Ashworth et al. (2001). Exchangeable NH_4^+ and NO_3^- were extracted using 2 M KCl at a 1:5 soil-to-solution ratio and quantified with a Skalar SAN^+ continuous flow analyzer (Amsterdam, Netherlands). Soil pH was assessed in a 1:2.5 soil-to-water suspension using a calibrated electrode (PHS-3C, Shanghai, China). Total C and N concentrations in soil were measured with an elemental analyzer (Multi N/C 3100, Jena, Germany).

2.4. Soil incubation and nitrification/denitrification potentials

To verify the observed decline in DMPP efficacy from the field trial, a 15-day laboratory incubation was conducted using soils collected from the F and F + DMPP plots at the end of the three-year experiment. The incubation comprised four treatments to disentangle the legacy effect of long-term field application from the immediate effect of a new DMPP dose on N_2O production: 1) F: soil from field F plot + 100 mg N kg^{-1} (urea), 2) F + DMPP: soil from field F plot + 100 mg N kg^{-1} + 1 % N DMPP, 3) F + Lab DMPP: soil from field F + DMPP plot + 100 mg N kg^{-1}, and 4) F + DMPP + Lab DMPP: soil from field F + DMPP plot + 100 mg N kg^{-1} + 1 % N DMPP. N_2O fluxes were monitored throughout the incubation (Li et al., 2022).

The potential for nitrification-derived N_2O emissions (NNP) was assessed by incubating soil samples for 24 h at 25 °C in a buffered NH_4Cl solution under continuous shaking. To distinguish the relative contributions of heterotrophic nitrifiers, AOA, and AOB, acetylene and 1-octyne were applied as selective inhibitors (Li et al., 2024; Taylor et al., 2015). Pre-experimental inhibitor tests [$(NH_4)_2SO_4$ with acetylene, 1-octyne, or DMPP] confirmed negligible Comammox contributions to NNP (Jiang et al., 2023; Fig. S2). Potential denitrification rates (PDR) were measured via acetylene (C_2H_2) inhibition (Smith and Tiedje, 1979), incubating soil with potassium nitrate, C sources, and 10 % C_2H_2 under anaerobic conditions (25 °C, 5 h), followed by N_2O analysis.

2.5. Molecular analyses of microbial functional groups

Genomic DNA was extracted from 0.25 g of fresh soil using the DNeasy PowerSoil Pro Kit (Qiagen Inc., Germany). DNA concentrations were measured with a Nanodrop ND-100 spectrophotometer (Thermo Scientific, USA). Quantitative PCR (qPCR) assays targeting functional genes associated with N cycling, including 16S rRNA, AOA, AOB, Comammox Clade A/B, *nir*K, *nir*S, and *nos*ZI, were conducted using the StepOnePlus™ Real-Time PCR System (Applied Biosystems). Detailed primer information and thermal cycling conditions are provided in Table S2. Each 20 μL reaction mixture contained 10 μL of SYBR® Premix Ex Taq, 0.4 μL of ROX reference dye (50 ×), 0.4 μL each of forward and reverse primers, 6.8 μL of ultrapure water, and 2 μL of template DNA. Amplification specificity was verified through melting curve analysis, and gene copy numbers were determined using standard curves.

To evaluate the long-term effects of DMPP application on ammonia-oxidizing and denitrifying communities, seasonal DNA samples (collected from 2020 to 2023 under the F and F + DMPP treatments) were subjected to high-throughput sequencing. Target genes included AOA, AOB, and *nos*Z. Sequencing reads were demultiplexed and processed in QIIME (Caporaso et al., 2010), with quality filtering performed via USEARCH. Operational taxonomic units (OTUs) were defined at a 97 % sequence similarity threshold and annotated according to the method described by Edgar (2013). Phylogenetic relationships among dominant AOB OTUs (relative abundance > 1 %) and reference sequences retrieved from the NCBI database were analyzed using MEGA X software, employing the neighbor-joining method with the Kimura 2-parameter model and 1000 bootstrap replicates (Kumar et al., 2018). All sequencing data have been submitted to the NCBI Sequence Read Archive under accession number PRJNA1266474.

2.6. Meta-analysis

We performed a global *meta*-analysis to evaluate the effects of DMPP on soil N_2O emissions and N-cycling functional genes. Peer-reviewed literature was retrieved from the Web of Science database using the keywords: "nitrous oxide" or "N_2O", "DMPP" or "3,4-dimethylpyrazole phosphate", and "soil". Eligible studies included field experiments covering full growing seasons with DMPP and control treatments. From 88 studies, 273 paired observations were extracted: 201 for N_2O emissions, 37 for ammonia oxidation genes (AOA and AOB), and 35 for denitrification genes (*nir*K, *nir*S, and *nos*Z; *nos*ZII merged due to limited data) (Fig. S3, Table S3). Effect sizes were computed using the natural logarithm of the response ratio as follows:

$$\ln R = \ln\left(\frac{X_t}{X_c}\right) \quad (4)$$

where *Xt* and *Xc* denote the mean values of total N_2O emissions or gene abundances for the treatment and control groups, respectively. To assign weights to individual observations, we applied a replication-based weighting scheme consistent with Wang et al. (2022):

$$Weight = \frac{N_c \times N_t}{N_c + N_t} \quad (5)$$

where N_c and N_t represent the number of replicates in the control and treatment groups. The overall effect size (mean ln*R*) and its 95 % confidence intervals (CIs) were estimated using the '*metafor*' package in R. An effect was considered statistically significant when the CIs did not overlap with zero.

2.7. Multivariate random forest regression modeling

To estimate the effectiveness of DMPP in mitigating N_2O emissions across global croplands, a Random Forest (RF) regression model was employed. This approach incorporated both environmental and management-related predictors, following the methodology described by Liu et al. (2019) and Prasad et al. (2006). Owing to the scarcity of grassland data (only 22 datasets), the model was exclusively applied to cropland data, including the data of uplands and paddy fields. The dataset included a range of explanatory variables, such as mean annual air temperature (MAT), mean annual precipitation (MAP), soil pH, clay percentage, SOC, C/N, N application rate, as well as the application rate and duration of DMPP treatment. Training data included 179 cropland observations (70 % training, 30 % testing; Fig. S4), with ln*R* (N_2O response ratio) as the dependent variable.

Global cropland N_2O emission variability under DMPP application was projected using a Random Forest (RF) model, integrating spatial datasets. Spatial data on soil properties at a resolution of 10 km^2 were obtained from the Harmonized World Soil Database (HWSD; https://daac.ornl.gov/SOILS/guides/HWSD.html). Climatic variables, including mean annual MAT and MAP, were retrieved from the WorldClim database (https://www.worldclim.org/) at the same spatial resolution. National-scale N application rates, averaged over the period 2019 to 2021, were sourced from the Food and Agriculture Organization of the United Nations (FAO) (https://www.fao.org/statistics/en/). DMPP efficacy was modeled at 0.9 % N application rate (mean rate of the dataset) and two durations, and then combined the other factors mentioned above to form two RF models for comparison. In the model, the duration of DMPP application was parameterized as two distinct scenarios: a short-term application (0.5-yr, 0.5 years, representing a single cropping season) and a long-term application (5-yr, 5 years, representing sustained use). Emission reductions were quantified by coupling RF outputs with global cropland N_2O data (2001–2020; Cui et al., 2021). To visualize the data more closely, we have presented continental-scale data from the model. All spatial maps were produced using ArcMap software (version 10.8, Esri, Redlands, CA, USA).

2.8. Statistical analysis

All datasets were assessed for normality using the Shapiro-Wilk test and for homogeneity of variances using chi-square analysis. Variables that did not meet the assumptions of normal distribution or equal variance were log-transformed prior to statistical analysis. Linear mixed-effects models were applied to evaluate temporal patterns in N_2O fluxes and soil physicochemical properties, with treatment included as a fixed effect and plot and sampling time treated as random effects. Post hoc comparisons were performed using Tukey's Honest Significant Difference (HSD) test. To examine differences in nitrification and denitrification potentials as well as functional gene abundances among treatments, non-parametric Kruskal-Wallis tests were employed. Microbial community composition was evaluated using non-metric multidimensional scaling (NMDS) based on Bray-Curtis dissimilarity matrices, allowing comparison across treatments and time points. Co-occurrence networks (Gephi 0.9.2) based on Spearman correlations visualized OTU interactions, with cohesion indices quantifying cooperative/competitive behaviors (positive/negative cohesion; Hernandez et al., 2021; Herren & McMahon, 2017). We constructed a RF model using the assembled database to explore the primary drivers of DMPP effectiveness in reducing N_2O emissions worldwide. To accurately assess the impact of climate, we used seasonal mean air temperature (Seasonal Temp) and seasonal precipitation (Seasonal Prec) to characterize climatic factors in the model. All statistical analyses were conducted in R software (version 4.2.2; R Core Team, 2021). Additional methodological details are available in the Supplementary Materials.

3. Results

3.1. N_2O emissions and environmental drivers

Across the experimental period, N_2O emissions from between-row soils exhibited consistent seasonal patterns across treatments, characterized by pulse-like peaks during spring and summer (Fig. 1a). The highest fluxes occurred in June or July each year, with maxima of 5636, 6194 and 4897 μg N m^{-2} h^{-1} observed in the F treatment, respectively. Peak emissions were closely associated with fertilization events and subsequent environmental changes. Peak emissions aligned with the second top-dressing fertilization, coinciding with elevated soil temperatures (26–29 °C) and WFPS levels of 45–52 % (Fig. S5). In contrast, the Control treatment maintained consistently low N_2O fluxes (< 950 μg N m^{-2} h^{-1}).

DMPP addition significantly mitigated peak fluxes, reducing emissions by 2142–4548 μg N m^{-2} h^{-1} over the three years. Correspondingly, cumulative emissions were reduced by 54 % (26 kg N ha^{-1}) in 2020–2021, but the mitigation effect declined to 39 % (15 kg N ha^{-1}) by 2022–2023 (Table 1, Fig. 1b). Linear mixed models confirmed a significant reduction in emissions during 2020–2022, but no statistical difference was detected in 2022–2023 (Table S4). Laboratory incubations further verified the diminished efficacy of DMPP in pre-treated soils, with DMPP-induced reductions in N_2O emissions declining from 45 % to 20 % over time (Fig. S6). Under-canopy emissions remained consistently low (< 800 μg N m^{-2} h^{-1}) and were unaffected by treatment (Fig. S7). The EFs for fertilized treatments ranged from 1.71 % to 2.39 %, with DMPP reducing EFs from 2.39 % to 1.02 % (a 1.37 % reduction) in 2020–2021 and from 1.83 % to 1.39 % (a 0.44 % reduction) in 2022–2023 (Table 1). Data gaps occurred during the post-fertilization period following the first top-dressing in 2021 due to COVID-19 restrictions (as detailed in Section 2.1), which may have led to an underestimation of the cumulative emissions and EFs for the 2021–2022 period.

Following the first top-dressing fertilization each year, soil NH_4^+ concentrations in between-row soils increased significantly, remaining elevated (200–400 mg N kg^{-1}) from April to August (Fig. 1d). NO_3^- concentrations exhibited a similar trend, though they lagged behind NH_4^+ increases (Fig. 1e). In the Control treatment, both NH_4^+ and NO_3^- remained consistently low, ranging from 2.8–46.2 mg N kg^{-1} for NH_4^+ and 4.2–66.3 mg N kg^{-1} for NO_3^-. Across fertilized plots, NH_4^+ concentrations were generally higher in the F + DMPP treatment (4.5–396.0 mg N kg^{-1}) than in the F treatment (2.1–325.3 mg N kg^{-1}). Conversely, NO_3^- concentrations were lower in the F + DMPP treatment (2.3–219.6 mg N kg^{-1}) relative to the F treatment (8.4–252.0 mg N kg^{-1}), with significant differences detected only in 2020–2021 ($p < 0.05$; Table S4). In under-canopy soils, NH_4^+ and NO_3^- concentrations remained low and were not significantly different between treatments (Fig. S8). Soil pH remained stable (4.0–6.0) across zones and treatments (Fig. 1c).

3.2. N_2O production potentials and functional gene abundances

Nitrification-derived N_2O potential (NNP) was initially low (< 15.0 μg N_2O-N kg^{-1}) following basal fertilization in winter 2020 but exhibited seasonal increases thereafter. DMPP application significantly reduced NNP by 65 % in summer 2021 and by 46 % in summer 2022, though its efficacy declined further by 2023 (Fig. 2a). Heterotrophic nitrification contributed 38–57 % of the total NNP across treatments, with no significant treatment effects (Fig. 2b).

After fertilizer application, the contribution of AOB to NNP in the

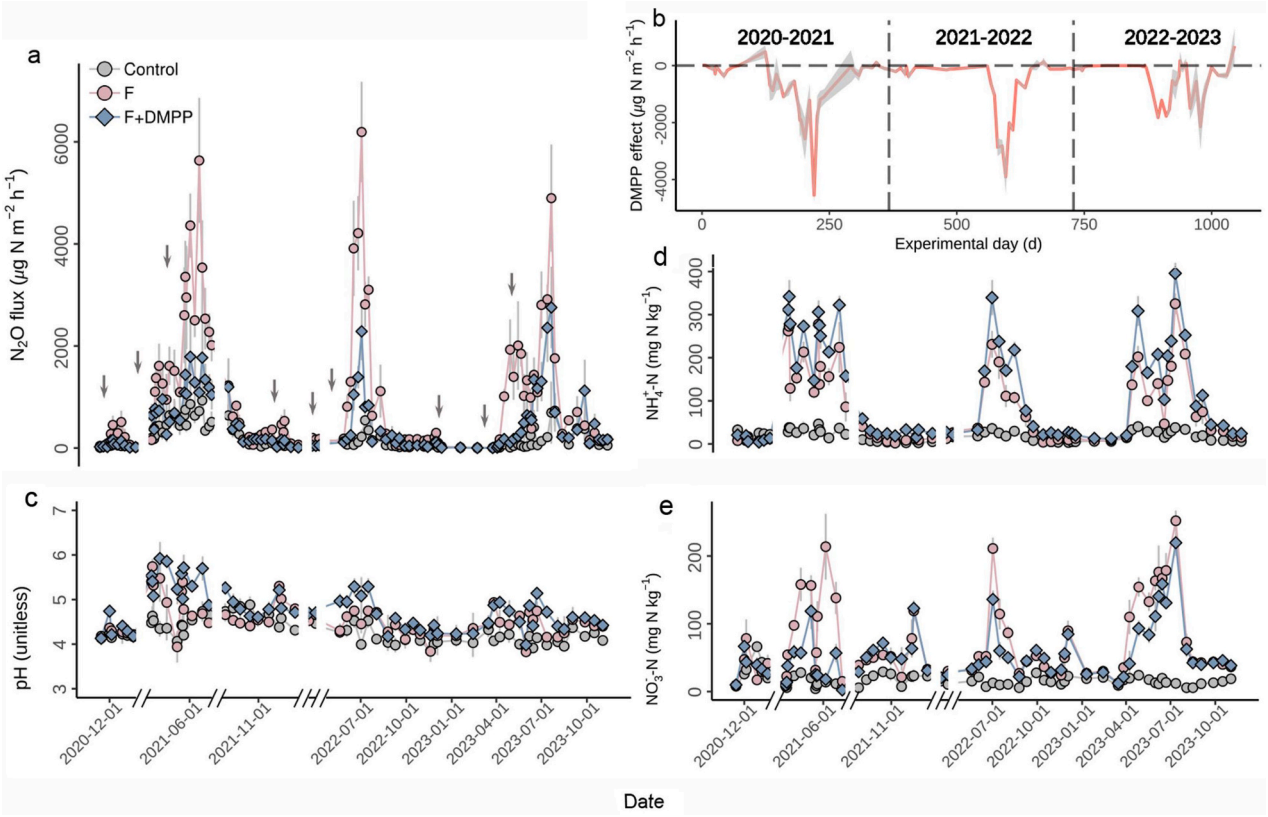

Fig. 1. Temporal variability of fluxes of N_2O (a), the amount of N_2O emission reduction attributable to DMPP application (b), soil pH (c), NH_4^+ (d), NO_3^- (e) from the soil between rows in a subtropical tea plantation. Error bars indicate the standard error (SE) of the mean (n = 3). Control, unfertilized plots; F, plots with conventional fertilization; F + DMPP, F plots with DMPP amendment. The downward arrows indicate dates of N fertilization. The truncations at the x-axis indicate the lack of sampling campaign during the lockdown period due to the COVID-19 pandemic.

Table 1
Emissions of soil N_2O and the emission factors (EF) from the acid tea plantation soils during the 2020–2023 experimental period.

	N_2O (kg N ha^{-1} $year^{-1}$)			EF (%)
Treatment	E_{rows}	E_{canopy}	Whole plot	
2020–2021				
Control	12.84 ± 2.67^b	8.61 ± 1.34^a	9.46 ± 1.56^b	
F	48.09 ± 5.24^a	13.30 ± 1.36^a	20.25 ± 0.82^a	2.39 ± 0.18
F + DMPP	22.19 ± 1.58^b	12.03 ± 1.81^a	14.06 ± 1.77^b	1.02 ± 0.39
2021–2022				
Control	3.91 ± 0.68^b	3.83 ± 0.95^a	3.85 ± 0.86^b	
F	33.60 ± 4.47^a	6.01 ± 0.64^a	11.52 ± 1.32^a	1.71 ± 0.29
F + DMPP	16.00 ± 1.27^b	6.02 ± 1.17^a	8.02 ± 1.16^b	0.70 ± 0.26
2022–2023				
Control	6.90 ± 0.67^c	5.76 ± 0.37^b	5.98 ± 0.16^c	
F	39.42 ± 3.43^a	7.94 ± 0.96^{ab}	14.24 ± 0.50^a	1.83 ± 0.11
F + DMPP	24.15 ± 1.77^b	9.99 ± 1.21^a	12.83 ± 0.73^b	1.39 ± 0.16

Note: E_{rows} and E_{canopy} represent N_2O emissions from the soil between rows and under the canopy, respectively. Values represent mean ± SE (n = 3). Control, unfertilized plots; F, plots with conventional fertilization; F + DMPP, F plots with DMPP amendment. Values with different lowercase letters for each column during each experimental period indicate significant differences between treatments at $p < 0.05$.

DMPP treatment decreased by 34 %, 17 %, and 15 % in 2021, 2022, and 2023, respectively, compared to the F treatment. In contrast, the relative contribution of AOA was consistently higher in the F treatment across most sampling periods, specifically by 31 % (2021-Summer), 14 % (2021-Winter), 10 % (2022-Summer), 13 % (2022-Winter), and 11 % (2023-Summer), with the exception of a comparable level observed in the initial 2020-Winter (Fig. 2b). Potential denitrification rates (PDR) exhibited sporadic treatment differences, with rates in the F treatment exceeding those in F + DMPP during the summer of 2021, while the opposite trend was detected in the winter of 2022. However, the N_2O/(N_2O + N_2) ratio remained stable at approximately 0.8 across all treatments (Fig. S9).

Across the three-year study period, bacterial gene abundance was highest in summer and significantly decreased by DMPP application in the summer of 2021 (Fig. 3a). The abundance of AOA ranged from 2.0e + 6 to 7.3e + 7 copies g^{-1} in the F + DMPP treatment and appeared higher than in other treatments, although the difference was not statistically significant (Fig. 3b). The abundance of AOB was reduced by 78 % in DMPP-treated soils during the summer of 2021, though this suppression effect diminished over time (Fig. 3c). The presence of Comammox was confirmed in the acidic tea plantation soils, with Clade A abundances ranging from 1.8e + 9 to 1.8e + 10 copies g^{-1}, and Clade B abundances ranging from 7.8e + 8 to 1.9e + 9 copies g^{-1} (Fig. 3d, e). The abundance of *nirK* was significantly higher in the F treatment, while the *nirS* gene abundance was more dominant in the F + DMPP treatment. The abundance of the *nos*Z gene ranged from 2.7e + 9 to 1.2e + 10 copies g^{-1} and exhibited no significant treatment differences, as did the (*nir*K + *nir*S)/*nos*Z ratio (Fig. 3f-h, S10).

3.3. Diversity and composition of functional gene communities

A total of 4,408 OTUs were identified for AOA at a 97 % similarity threshold. The alpha diversity of AOA increased over time but remained unaffected by treatments (Fig. 4a). Correspondingly, NMDS analysis indicated that the AOA community composition did not differ significantly across treatments, although it shifted temporally (Fig. 4b). This

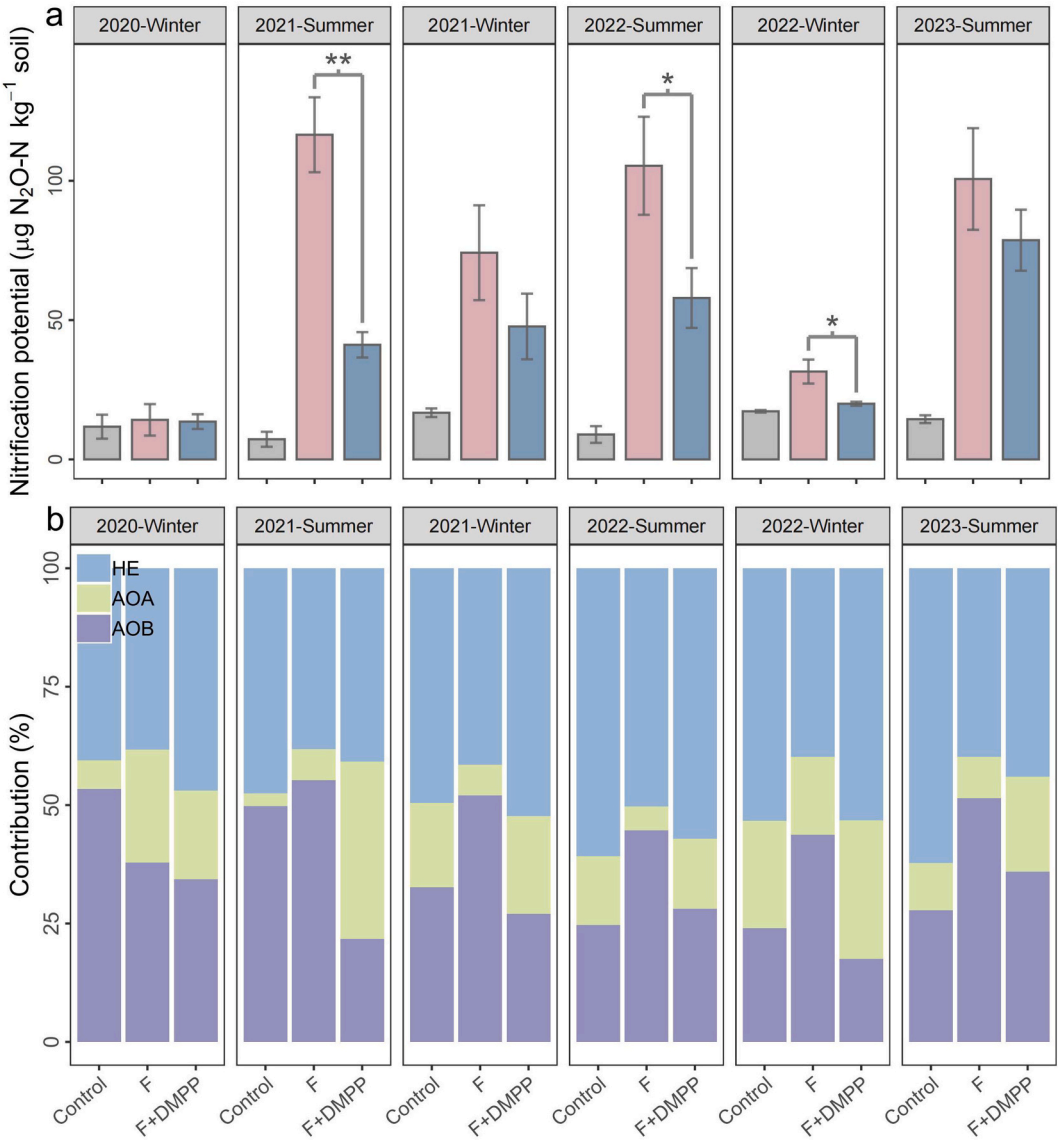

Fig. 2. Nitrification-derived N_2O potentials (a) and the relative contribution of different pathways (b) for each treatment at different periods. HE, AOA, and AOB represent the relative contribution of heterotrophic nitrification, AOA, and AOB, respectively. Error bars indicate the mean's standard error (SE) (n = 3). For treatment abbreviations, see Fig. 1 legend. The special symbols assign a significance level between indicators from F and F + DMPP treatments. *$p < 0.05$, **$p < 0.01$.

temporal shift involved a transition from the initial dominance of *Candidatus Nitrosotalea* to an increasing dominance of *Nitrososphaera*, particularly in the F + DMPP treatment (Fig. 5a). Additionally, the abundance of *Candidatus Nitrosocosmicus* was significantly higher in DMPP-treated soils.

For AOB, 5,851 OTUs were identified. DMPP application significantly reduced AOB alpha diversity in the summer of 2021 ($p < 0.05$), though this effect was not observed in subsequent years (Fig. 4c). In contrast to AOA, the AOB community composition clustered distinctly according to both treatment and time point (Fig. 4d). The community was initially dominated by *Nitrosospira*, but in later stages, the relative proportion of *Nitrosomonas* increased significantly in the F + DMPP treatment (Fig. 5b). Given that *Nitrosospira* and *Nitrosomonas* accounted for approximately 99 % of the community, we conducted a detailed phylogenetic analysis. At the experiment's start (2020-Winter), AOB communities were primarily composed of *Nitrosospira* cluster 2/4 (60–78 %; Fig. 5d). After urea application, *Nitrosospira* cluster 3a.2 became dominant, but its proportion remained significantly higher in the F treatment than in F + DMPP in 2021-Summer (83 % *vs.* 41 %). By 2022–2023, a substantial increase in *Nitrosomonas* cluster 7 was observed in the F + DMPP treatment (23–25 %), whereas it was nearly absent in the F treatment.

The *nosZ* gene exhibited the highest diversity, with 12,008 OTUs identified. Significant differences in its species diversity and the Chao1 index were detected between the F and F + DMPP treatments ($p < 0.05$; Fig. 4e). NMDS ordination revealed that the *nosZ* community exhibited significant separation between treatments but not across different sampling periods (Fig. 4f). Compared to AOA and AOB, the *nosZ* community demonstrated greater taxonomic diversity and complexity (Fig. S11).

3.4. Co-occurrence networks of functional gene communities

Co-occurrence network analysis was conducted to examine associations among functional gene OTUs, with visualization limited to strong ($r > 0.7$) and statistically significant ($p < 0.01$) correlations. The AOA network exhibited distinct temporal shifts in connectivity. During 2020–2021, DMPP application reduced both the number of nodes and edges. However, by 2022–2023, AOA network complexity increased substantially, with the number of edges rising from 854 to 3,204 and the

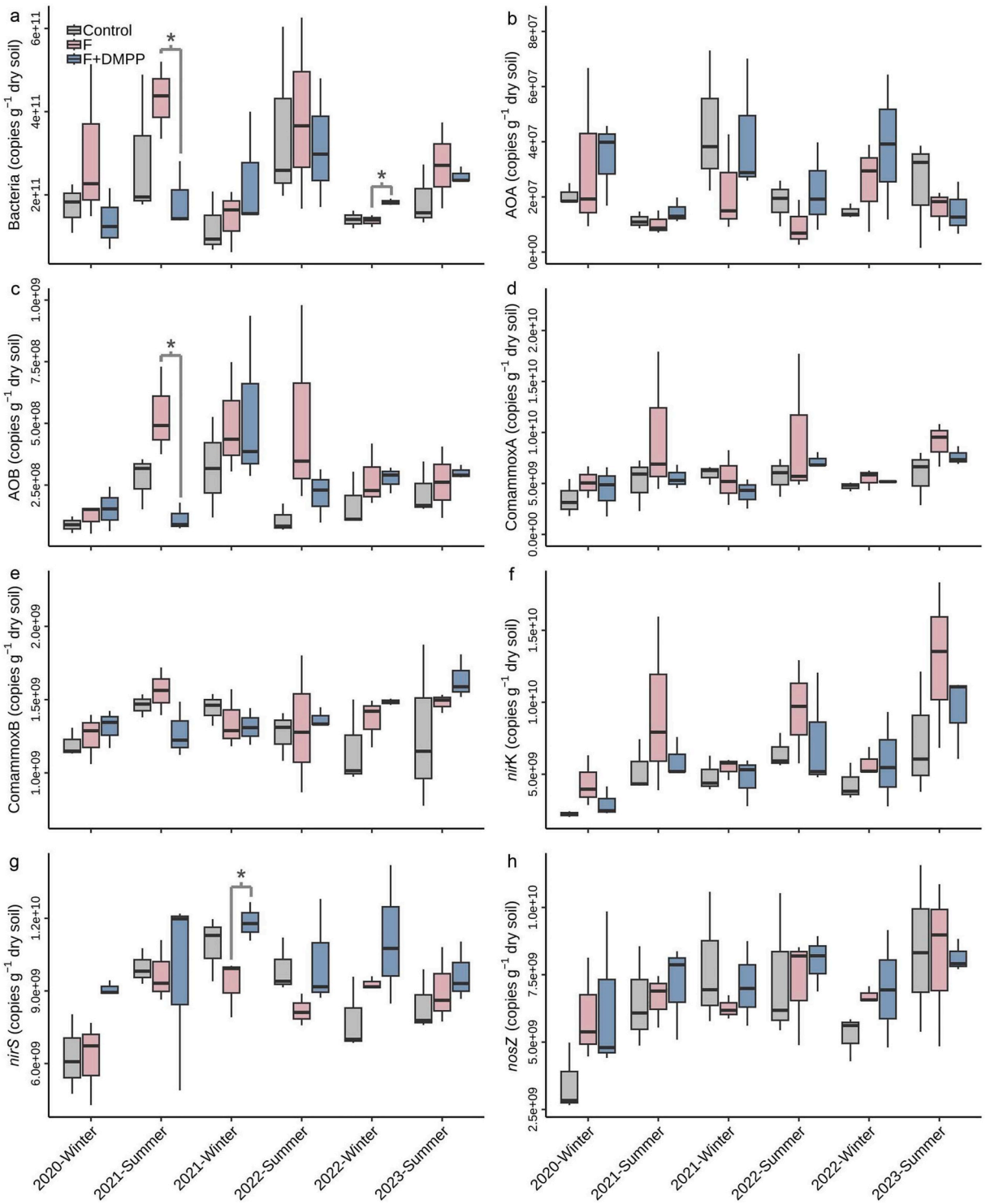

Fig. 3. Abundance of bacteria and functional genes associated with the N cycle in different fertilizer treatments at different periods (AOA, AOB, Comammox clade A, Comammox clade B, *nir*K, *nir*S, *nos*Z). For treatment abbreviations, see Fig. 1 legend. The special symbols assign a significance level between indicators from F and F + DMPP treatments, $^{*}p < 0.05$.

number of nodes increasing from 161 to 265 (Fig. 6a). Unlike AOA, the AOB network exhibited higher connectivity during 2020–2021, with 3,904 edges and 366 nodes. DMPP applications significantly reduced network complexity in both experimental periods (Fig. 6b). Moreover, the average degree of AOB network connectivity was lower under DMPP treatment, whereas network modularity was higher, suggesting an increase in community compartmentalization (Table S5). Compared to AOA and AOB, the *nosZ* network exhibited less pronounced responses to DMPP treatment, although both the number of edges and nodes increased over time (Fig. 6c).

To further elucidate the structural stability of these networks, we calculated cohesion metrics. Positive cohesion for AOA did not differ significantly among treatments; however, in 2020–2021, negative cohesion was significantly lower in the F + DMPP treatment compared to the F treatment ($p < 0.01$), resulting in a lower total cohesion ($p < 0.01$; Fig. 6d). Similar to the results observed for AOA, the positive

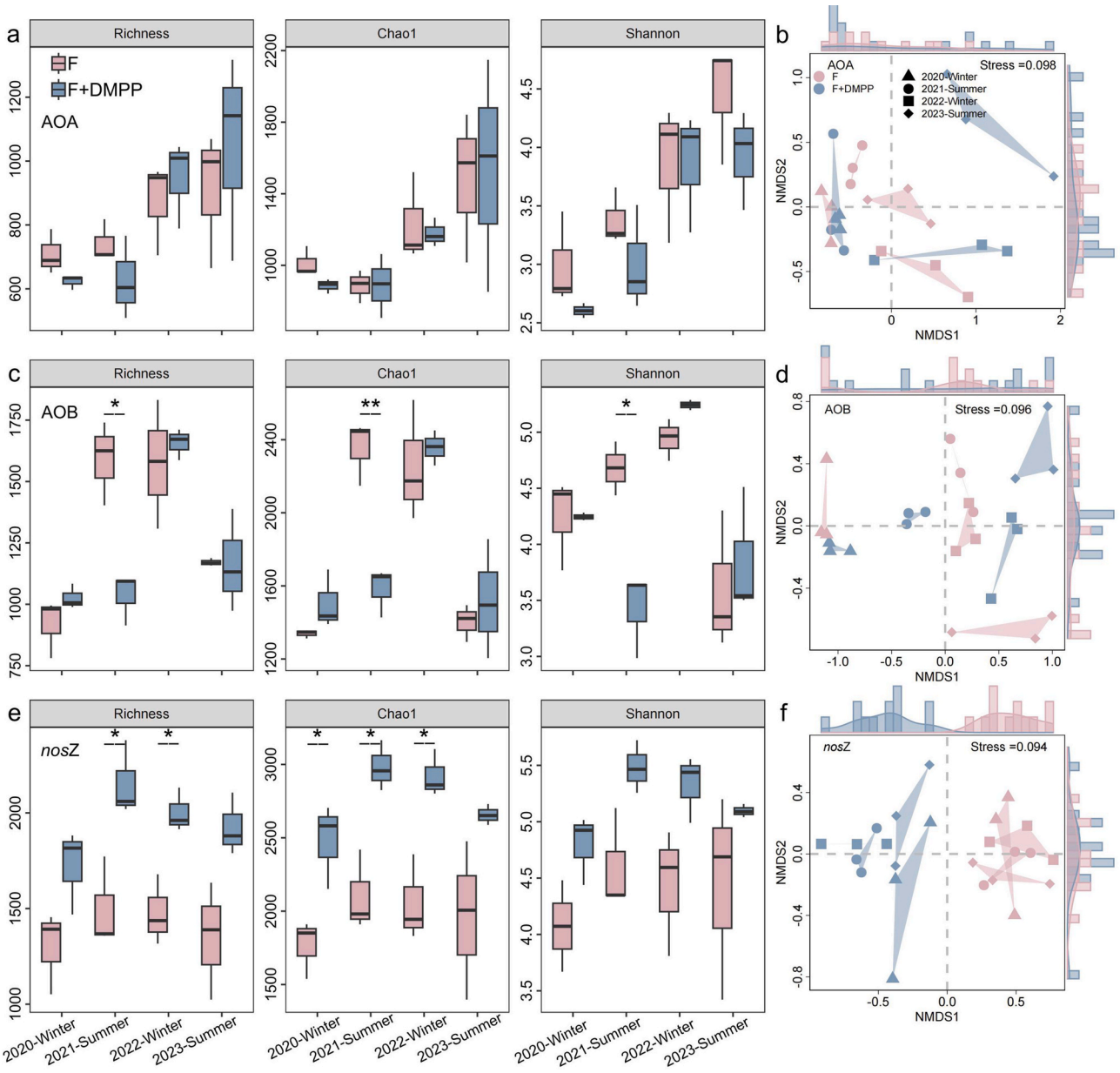

Fig. 4. The alpha diversity (Species richness, Chao1 index, and Shannon index) and the NMDS ordination plot for distribution analysis of AOA (a and b), AOB (c and d) and *nos*Z-bearing bacteria (e and f) among the different fertilizer treatments and different periods. For treatment abbreviations, see Fig. 1 legend. The special symbols assign a significance level between indicators from F and F + DMPP treatments. *$p < 0.05$, **$p < 0.01$.

cohesion within AOB co-occurrence networks did not differ significantly among treatments (Fig. 6e). In contrast, negative cohesion was consistently and significantly greater in the F + DMPP treatment compared to the F treatment across both sampling periods ($p < 0.01$). This was accompanied by a significant increase in the |Negative|/Positive ratio under F + DMPP ($p < 0.01$). In contrast, the *nosZ* network exhibited increased negative cohesion in the F treatment during 2022–2023 ($p < 0.01$; Fig. 6f), suggesting distinct regulatory dynamics between denitrification-associated microbial communities.

3.5. Global N_2O response to DMPP and key drivers

A *meta*-analysis of 201 paired observations from 88 field studies (Fig. 7a) revealed that DMPP application significantly reduced N_2O emissions, with a ln*R* of −0.68 (95 % CIs: −0.79 to −0.56; Fig. 7b). When stratified by land-use type, the mean lnR values for upland, paddy, and grassland soils were −0.68 (95 % CIs: −0.80 to −0.56), −1.01 (95 % CIs: −1.40 to −0.62), and −0.44 (95 % CIs: −0.75 to −0.13), respectively, indicating that DMPP was most effective in paddy soils. The application of DMPP led to a significant reduction in AOB abundance, as indicated by a mean ln*R* of −0.37 (95 % CIs: −0.63 to −0.10). In contrast, field conditions showed no significant changes in the abundances of AOA, *nir*K, *nir*S, or *nos*Z genes (Fig. 7c).

The RF model identified SOC content and DMPP application duration as the most influential factors controlling the magnitude of N_2O reduction (Fig. 7d). Meta-regression analysis revealed that the ln*R* of N_2O emissions was positively associated with SOC content ($p < 0.01$; Fig. 7e) and negatively associated with soil pH ($p < 0.001$; Fig. 7h). Beyond soil properties, seasonal mean air temperature (Seasonal Temp) emerged as a significant climatic driver of the N_2O mitigation effect ($p < 0.05$; Fig. 7g). Furthermore, the duration of DMPP application exhibited a significant negative correlation with ln*R* values ($p < 0.05$; Fig. 7f). The relationship between DMPP application rate and ln*R* followed a non-linear trend ($p < 0.01$; Fig. 7i), with the greatest mitigation effect

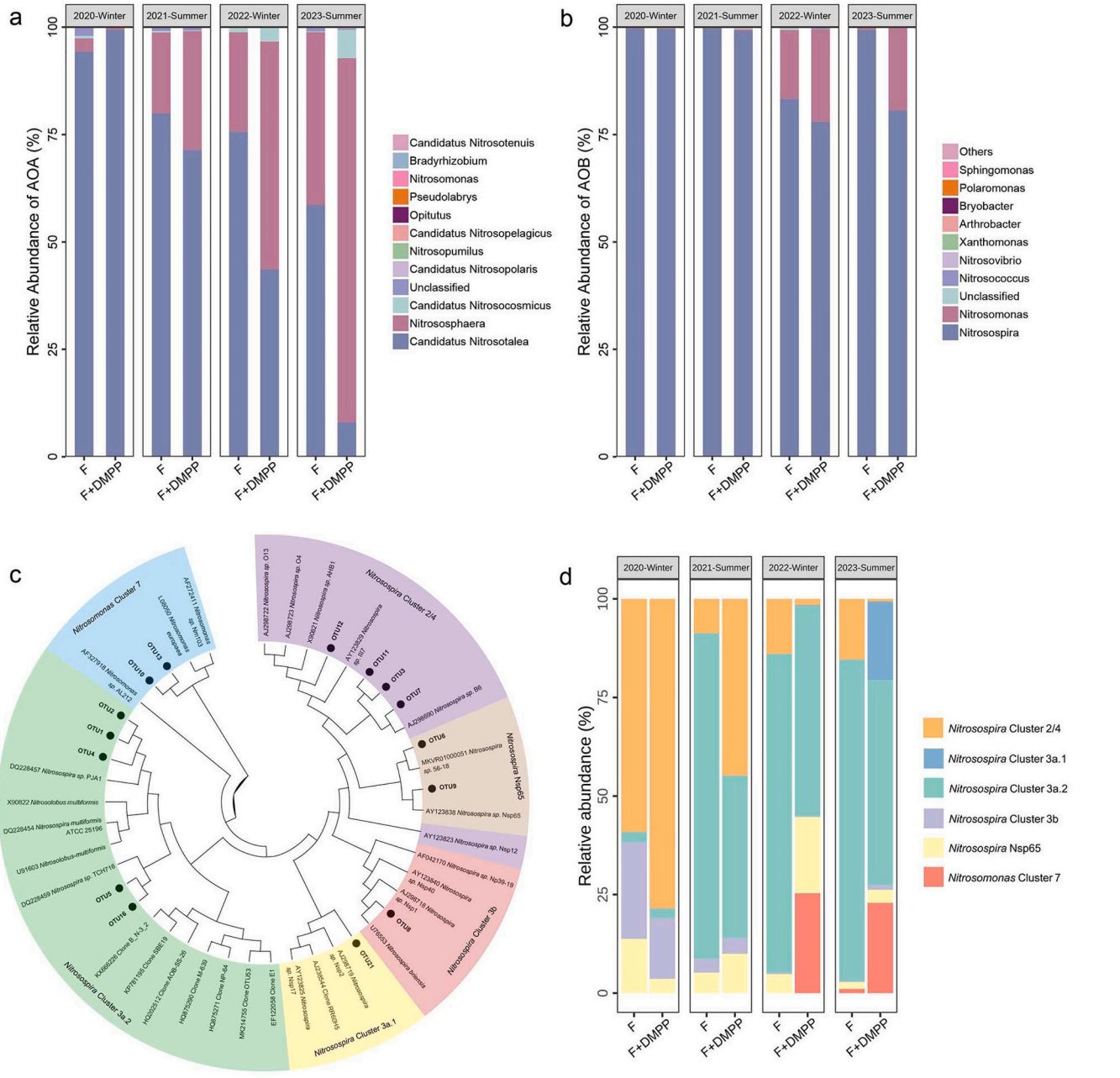

Fig. 5. Relative abundances of AOA (a) and AOB (b) microbial community composition at the genus level. Neighbor-joining tree for dominant AOB OTUs (OTU abundance > 1 %; c). AOB OTU representative sequences from this study are shown in bold. The relative abundance of AOB phylotypes among different treatments at different periods based on sequences (d). For treatment abbreviations, see Fig. 1 legend.

observed at an optimal rate of 1–2 % N.

3.6. Global prediction of DMPP mitigation potential

To assess the large-scale impact of DMPP application, we projected the trained RF model onto a global cropland dataset, generating predictions for short-term (0.5-yr) and long-term (5-yr) application scenarios (Fig. 8a, c). The results indicated that DMPP reduced global cropland N_2O emissions by an average of 61 % under the 0.5-yr scenario, but this mitigation effect declined to 50 % after 5 years of continuous application. Regionally, the highest N_2O mitigation was observed in Africa and Australia, where reductions reached nearly 70 % in the 0.5-yr scenario and approximately 58 % in the 5-yr scenario (Fig. 8e). In contrast, Europe exhibited the weakest mitigation response, with reductions of 53 % and 43 % under the respective application durations. The coefficient of variation for spatial variability estimates was 34 % and 30 % for the two prediction models, respectively (Fig. S12).

Further quantitative assessments estimated that, given an annual N_2O emission of 1000 Gg N yr^{-1} from cropland N fertilization, DMPP application could reduce emissions by 591 and 494 Gg N yr^{-1} under the 0.5-yr and 5-yr scenarios, respectively (Fig. 8b, d). Intercontinental comparisons revealed that N_2O mitigation potential declined with prolonged DMPP use (Fig. 8f). Asia demonstrated the highest mitigation potential, with reductions of 294 Gg N yr^{-1} and 248 Gg N yr^{-1} in the 0.5-yr and 5-yr scenarios, respectively. China accounted for nearly 40 % of these reductions, underscoring its critical role in global N_2O mitigation efforts.

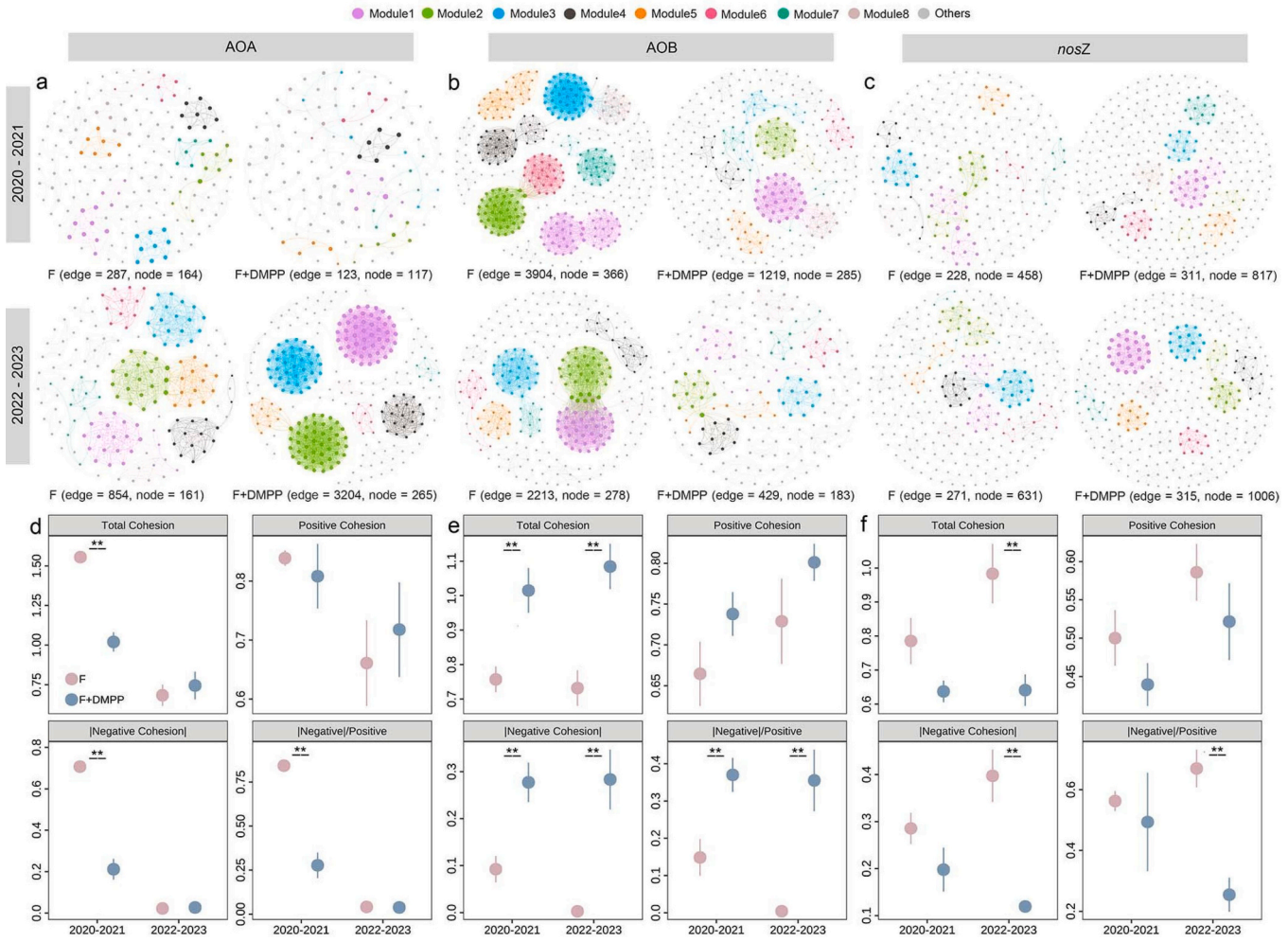

Fig. 6. Co-occurrence networks of AOA (a), AOB (b) and *nosZ* (c) from the different fertilizer treatments at different periods based on OTU profiles. Effects of DMPP application on total cohesion, positive cohesion, negative cohesion and ratio of negative to positive cohesion of AOA (d), AOB (e) and *nosZ* (f). For treatment abbreviations, see Fig. 1 legend. The special symbols assign a significance level between indicators from F and F + DMPP treatments. $^{**}p < 0.01$.

4. Discussion

4.1. Weakened N_2O mitigation under consecutive applications of DMPP

Results from our multi-year field experiment demonstrated that DMPP was effective in reducing N_2O emissions during the initial two years; however, its mitigation efficacy diminished with prolonged application, a phenomenon governed by adaptive microbial ecological feedbacks. This declining efficiency is not merely an agronomic concern but signifies a fundamental shift in soil microbial ecology with direct consequences for the environmental sustainability of nitrification inhibition strategies. On average, DMPP application reduced N_2O emissions by 48 % in the inter-row areas and consistently lowered the field-scale EF over the three-year observation period (Fig. 1a), aligns with the previous study reporting the effectiveness of NIs in suppressing N_2O emissions (Yamamoto et al., 2014). However, the temporal decay of this effect (Fig. 1b), corroborated by diminishing differences in soil NH_4^+ and NO_3^- dynamics (Fig. 1d-e, Table S4), points to a loss of inhibitory potency, likely driven by microbial adaptation. Unlike studies attributing DMPP variability to climatic extremes (Dong et al., 2021), our field conditions remained relatively stable, with no extreme rainfall or drought events, and WFPS levels held consistent across years (Fig. S5). Laboratory incubations confirmed that soil properties intrinsic to the tea plantation likely played a dominant role in the observed attenuation (Fig. S6).

Our findings confirm our first hypothesis that sustained DMPP application reshapes nitrifier community structure and function, ultimately undermining its mitigation efficacy. The mechanism centers on a dual ecological response within the ammonia-oxidizing community. First, a suppression-and-compensation dynamic between AOB and AOA. While DMPP initially and effectively suppressed AOB abundance and their contribution to the nitrification-derived N_2O potential (NNP) (Fig. 2b and 3c), this created a competitive release for AOA, leading to their increased relative contribution (Fig. 2b). However, it is critical to note that AOA intrinsically possess a much lower N_2O yield per cell than AOB (Hink et al., 2017). This means that the observed increase in AOA relative abundance would need to be quantitatively very large to fully compensate for the loss of N_2O production from the inhibited AOB population. Critically, the AOA community shifted towards taxa like *Nitrososphaera* and *Candidatus Nitrosocosmicus* (Fig. 5a), which are known for their high N_2O yield and ammonium tolerance, thereby compensating for the inhibited nitrification activity but with a potentially higher N_2O emission from nitrification (Lehtovirta-Morley et al., 2016; Stieglmeier et al., 2014). This compensation mechanism effectively creates an ecological trade-off: the very suppression of the primary target (AOB) inadvertently promotes a secondary, less-sensitive nitrifying pathway (AOA) that may sustain N_2O production even under inhibition. Furthermore, the progressive soil acidification observed under high N input likely acted synergistically with DMPP to shape the microbial community (Fig. 1c). The declining pH inherently favors acid-

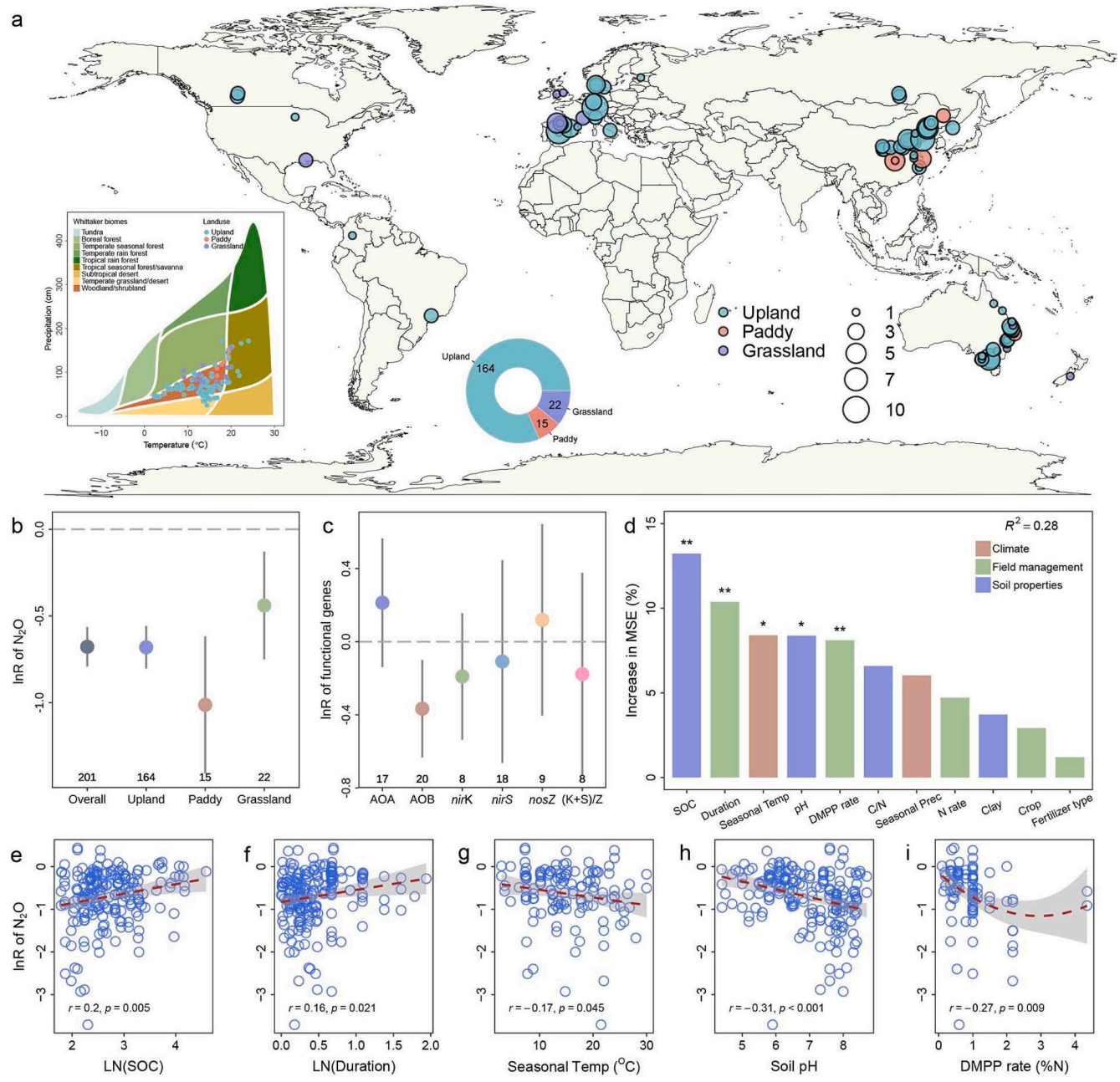

Fig. 7. Global distribution of field studies measuring N_2O emissions after DMPP application (a). The size of the dots denotes the number of N_2O measurements and differentiates between various land use types. The natural log-transformed response ratios (ln*R*) of soil N_2O emissions (b) and related functional gene abundances to DMPP application based on the global database (c), the upper and lower error bars indicate 95 % confidence intervals. The number of observations is given for each index. The dotted line is drawn at zero. The random forest model importance of different factors for ln*R* of DMPP efficacy on soil N_2O emissions (d) and the *meta*-regression between the ln*R* and SOC (e)/DMPP application duration (f)/seasonal mean air temperature (g)/soil pH (h)/DMPP application rate (i). * $p < 0.05$, ** $p < 0.01$.

tolerant AOA over AOB (Nicol et al., 2008), thereby reinforcing the competitive release of AOA and accelerating the formation of a DMPP-resilient nitrifying consortium.

Second, and more profoundly, we observed an adaptive restructuring within the AOB community itself. The initial suppression of AOB alpha diversity (Fig. 4c) was followed by a compositional shift from DMPP-sensitive *Nitrosospira* cluster 3a.2, which is a key contributor to N_2O emissions and the primary target of DMPP (Bai et al., 2023; Zhong et al., 2016), toward the enrichment of *Nitrosomonas* cluster 7 (Fig. 5). This shift is pivotal, as *Nitrosomonas* is recognized for its role in N_2O production and appears to exhibit lower sensitivity to DMPP in this system, as previously suggested in biochar-amended soils (Lin et al., 2017). The co-occurrence network analysis further reveals that these taxonomic changes occurred alongside intensified competitive interactions within the AOB community (evidenced by increased negative cohesion; Fig. 6e). Collectively, this demonstrates a process of microbial selection for N_2O-productive nitrifier lineages that can thrive under the selective pressure of sustained DMPP application. The ecological implications of this microbial adaptation are significant. The transition of the nitrifier community towards AOA and AOB taxa with higher inherent N_2O-producing potential means that even a partially inhibited nitrification process could sustain substantial N_2O emissions. This functional redundancy and niche compensation explain the observed decline in DMPP's mitigation efficiency over time. This pattern mirrors the

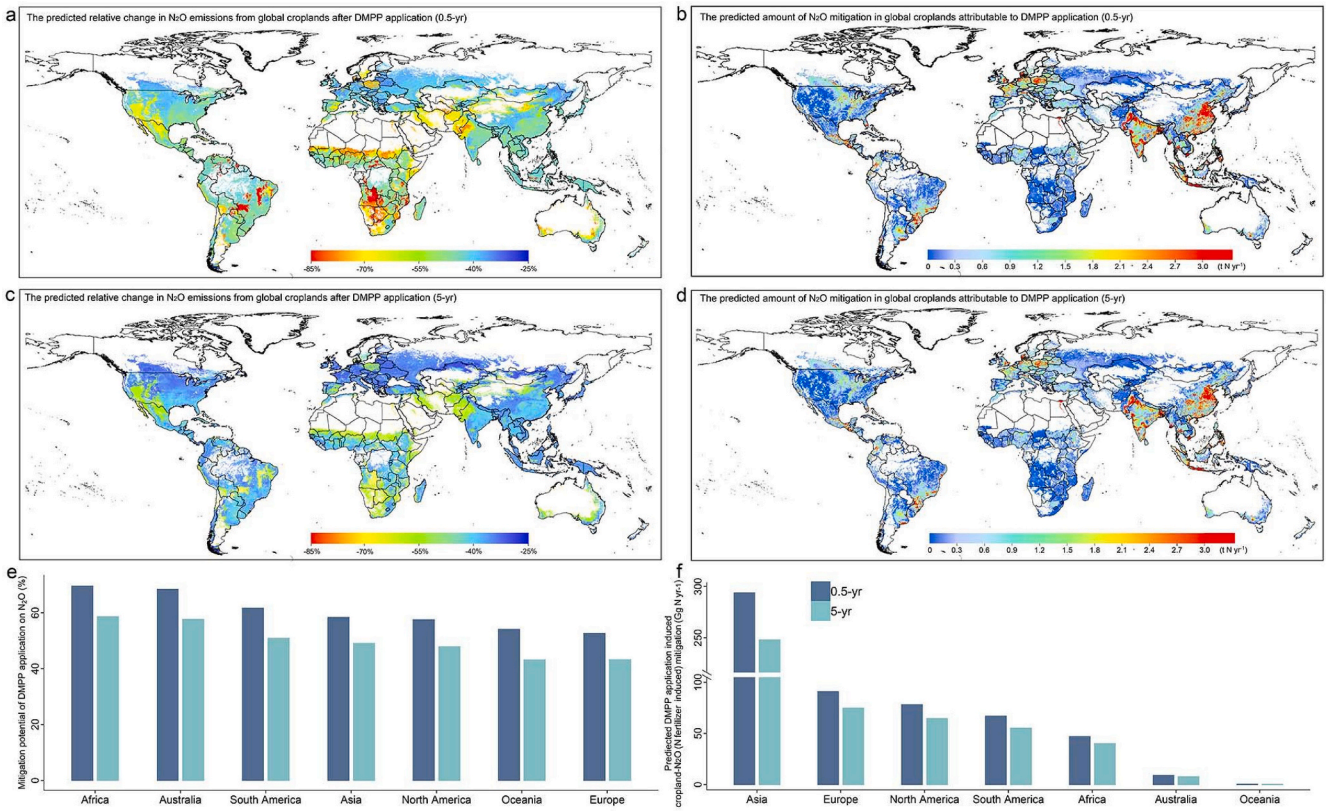

Fig. 8. Spatial patterns of N_2O mitigation efficiency and mitigation amount for DMPP application, a-b: the scenario of applying DMPP for half a year (0.5-yr model); c-d: the scenario of applying DMPP for five years (5-yr model). The comparison of DMPP-induced mitigation efficiency (e) and mitigation amount among continents (f) in the 0.5-yr and 5-yr models.

evolution of resistance to pesticides and antibiotics, where sustained chemical pressure selects for tolerant lineages, thereby diminishing the intervention's long-term effectiveness (Allison and Martiny, 2008; Andersson and Hughes, 2010). Notably, a recent study under repeated exposure regimes confirmed that while DMPP's inhibitory efficacy remained stable, it induced broad off-target effects on the soil microbial community, reinforcing that its long-term use imposes significant selective pressure beyond the intended nitrifier targets (Amanatidou et al., 2025). Therefore, the decrease in DMPP efficiency over time is indeed problematic for the soil microbial community, as it signifies a dysbiosis that selects for a more resilient nitrifying consortium.

While the adaptation of ammonia oxidizers provides a core explanation for the observed mitigation decay, a complete understanding of the N_2O flux under sustained inhibition requires future work on other key N-cycling groups. The functional role of comammox, despite its high abundance here and elsewhere (Jiang et al., 2023), remains unclear under long-term DMPP exposure. Concurrently, the significant shifts in the diversity and network structure of *nosZ*-type denitrifiers (Fig. 4e, 4f, and 6f) suggest a potential alteration of the N_2O consumption potential that warrants further investigation, especially given its documented importance (Friedl et al., 2020). We also acknowledge that data gaps during COVID-19 lockdowns may have led to an underestimation of cumulative emissions for the 2021–2022 period. However, this potential underestimation does not invalidate the clear temporal trend of declining efficacy observed across three full years, nor does it affect the mechanistic insights derived from our microbial community data.

4.2. *Duration-dependent efficacy of DMPP at global scale*

Building upon the mechanistic understanding of microbial adaptation from our field trial, our *meta*-analysis and RF modeling confirm that the declining efficacy of DMPP is a verifiable and predictable phenomenon across global croplands, thereby supporting our second hypothesis. On average, DMPP application reduced soil N_2O emissions by 49 % (Fig. 7b; 43 %-55 %), aligning with our experimental findings. This reduction is notably lower than the results reported in two recent *meta*-analyses, which found reductions ranging from 56 % to 71 % (Fan et al., 2022), can be attributed to our database's exclusive inclusion of field studies. This suggests that controlled laboratory conditions, which lack the complex ecological feedbacks observed in the field, may overestimate the real and long-term potential of DMPP (Tufail et al., 2022). Our field-informed approach thus provides a more conservative and likely more realistic assessment of the technology's durable impact. Additionally, our *meta*-analysis revealed that among N cycle functional genes, DMPP only significantly inhibited AOB (Fig. 7c), consistent with our experimental findings. Recent *meta*-analytic evidence also underscored the importance of AOB in predicting NI efficiency (Lei et al., 2022).

Our global prediction, the first to incorporate the duration of application, quantitatively affirms that long-term (5-yr) DMPP use results in a lower mitigation potential compared to short-term (0.5-yr) application (Fig. 8). This model output provides a crucial cross-scale validation of our field-based findings. The duration of consecutive DMPP application was identified as a key determinant of its efficacy (Fig. 7d), with a significant positive correlation between application duration and the ln*R* of N_2O (Fig. 7f). This global pattern of 'mitigation decay' directly mirrors and is mechanistically explained by the microbial adaptive processes which documented in the field: the progressive restructuring of the AOB community and the compensatory rise of N_2O-productive AOA (as detailed in Section 4.1). Here, 'duration' specifically refers to the number of consecutive years during which DMPP was applied, and our findings demonstrate that this continuous selective pressure is a primary driver of efficacy loss both locally and globally.

Other factors, including SOC, soil pH, and seasonal temperature,

were also important (Fig. 7e, g-i). The spatial variation in mitigation efficiency among continents (Fig. 8e) can be explained by the interplay of these environmental drivers. For instance, the lower mitigation efficiency in Europe may be linked to its generally higher SOC content, which can adsorb DMPP and reduce its bioavailability (Barth et al., 2008; Fisk et al., 2015), while the higher efficiency in Africa and Australia could be associated with their predominantly alkaline soils, where AOB, which is the primary target of DMPP, are more dominant (De Boer and Kowalchuk, 2001). Although Asia did not exhibit the highest mitigation efficiency, it holds the greatest absolute mitigation potential due to its vast fertilizer-induced N_2O emissions (Fig. 8f). This underscores that the environmental and agronomic implications of DMPP adaptation will be most acute in regions with intensive N fertilization. At the global scale, we estimate that DMPP application could reduce N_2O emissions by 494 to 591 Gg N yr^{-1}. While these estimates surpass certain agronomic mitigation thresholds (Cui et al., 2021), it is crucial to recognize that they represent a theoretical potential. The progressive decline in efficacy, as mechanistically explained by microbial adaptation, implies that these benefits are not sustainable under continuous and single agronomic management.

Given the inevitability of microbial adaptation, our findings compel a strategic shift in how NIs are deployed. To counteract the "mitigation decay" effect and extend the functional lifespan of NIs, we propose adopting resistance management principles. This could involve rotating or combining NIs with different molecular targets to reduce selective pressure, employing precision application guided by soil properties and microbial profiles to avoid blanket use, and integrating NI use with soil health practices (e.g., biochar) to create a less selective environment. Such an integrated approach is crucial to sustain long-term N_2O mitigation and preserve agroecosystem resilience.

5. Conclusion

Our field experiment and global *meta*-analysis provide two key insights into the long-term sustainability of NI strategies. First, consecutive DMPP applications triggered microbial adaptation through functional redundancy and niche partitioning, progressively diminishing its efficacy in mitigating N_2O. This adaptation was driven by a dual mechanism: high-N_2O-yielding AOA taxa (*Nitrososphaera* and *Candidatus Nitrosocosmicus*) compensated for suppressed AOB activity, while AOB communities shifted from *Nitrosospira* to DMPP-tolerant *Nitrosomonas* lineages. Second, our global assessment revealed a "mitigation decay" effect, where DMPP efficacy declined after five years of sustained use. Despite this decline, strategic deployment could still achieve global N_2O emission reductions of 494–591 Gg N yr^{-1}, with Asia contributing over 50 % of this potential. Drawing inspiration from microbial resistance management in pesticide and antibiotic applications, we propose a "NI rotation-combination" approach–alternating or co-applying inhibitors targeting both AOA and AOB, integrating urease inhibitors, and employing precision application guided by real-time microbial profiling to avoid indiscriminate use. Coupling these strategies with soil health interventions (e.g., biochar amendments) could sustain long-term N_2O mitigation while preserving agroecosystem resilience and fostering sustainable agricultural development.

CRediT authorship contribution statement

Zhutao Li: Writing – original draft, Visualization, Software, Methodology, Investigation, Formal analysis, Data curation. **Roland Bol:** Writing – review & editing. **Pinshang Xu:** Writing – review & editing, Investigation. **Zhaoqiang Han:** Writing – review & editing, Funding acquisition. **Jie Wu:** Writing – original draft, Methodology. **Xiang Gao:** Writing – review & editing. **Shumin Guo:** Writing – review & editing, Methodology. **Xiaomeng Bo:** Writing – review & editing, Investigation. **Haiyan Lin:** Writing – review & editing, Investigation. **Mengxue Shen:** Investigation. **Zhiwei Zhang:** Writing – review & editing, Investigation. **Zhe Xu:** Writing – review & editing. **Jinyang Wang:** Writing – review & editing, Supervision, Funding acquisition, Conceptualization. **Jianwen Zou:** Writing – review & editing, Supervision, Funding acquisition, Conceptualization.

Declaration of competing interest

The authors declare that they have no known competing financial interests or personal relationships that could have appeared to influence the work reported in this paper.

Acknowledgments

This work was supported by the National Natural Science Foundation of China (Grant Nos. 42477358, 42407472, and 42177285) and the Fundamental Research Funds for the Central Universities (Grant No. KJYQ2025037). This research was also partially supported by the initiative advancing dual certification for eco-friendly premium agricultural products and carbon footprint assessment launched by the Green Food Office of the Jiangsu Provincial Department of Agriculture and Rural Affairs. We are grateful to Longzheng Wang, Jiancheng Qi, Genyuan Liu, Haochen Zheng, and Lei Wang for their valuable assistance with field sampling and laboratory analyses. We also thank Prof. Feng Zhou and Dr. Xiaoqing Cui for providing access to the global cropland N_2O emission raster dataset.

Appendix A. Supplementary material

Supplementary data to this article can be found online at https://doi.org/10.1016/j.geoderma.2025.117641.

Data availability

Data will be made available on request.

References

Abalos, D., Sanz-Cobena, A., Andreu, G., Vallejo, A., 2017. Rainfall amount and distribution regulate DMPP effects on nitrous oxide emissions under semiarid Mediterranean conditions. Agric. Ecosyst. Environ. 238, 36–45. https://doi.org/10.1016/j.agee.2016.02.003.

Akiyama, H., Sasaki, Y., Tago, K., Wang, Y., Hayatsu, M., 2025. Mitigation of nitrous oxide emissions by 3,4-dimethylpyrazole phosphate and 3,4-dimethylpyrazole succinic acid with reduced fertilizer application time while maintaining cabbage yield in Andosol fields. Agric. Ecosyst. Environ. 393.

Allison, S.D., Martiny, J.B.H., 2008. Resistance, resilience, and redundancy in microbial communities. Proc. Natl. Acad. Sci. USA 105, 11512–11519. https://doi.org/10.1073/pnas.0801925105.

Amanatidou, P., Perruchon, C., Mavrou, E., Moutzourelli, C., Karpouzas, D.G., Papadopoulou, E.S., 2025. Dicyandiamide (DCD) and 3,4-dimethylpyrazole phosphate (DMPP) demonstrate distinct inhibitory activity, dissipation patterns and off- target effects in soils under repeated exposure regimes. Biol. Fertil. Soils 61, 1253–1269.

Andersson, D.I., Hughes, D., 2010. Antibiotic resistance and its cost: is it possible to reverse resistance? Nat. Rev. Microbiol. 8, 260–271. https://doi.org/10.1038/nrmicro2319.

Ashworth, J., Keyes, D., Kirk, R., Lessard, R., 2001. Standard procedure in the hydrometer method for particle size analysis. Commun. Soil Sci. Plant Anal. 32, 5–6. https://doi.org/10.1081/CSS-100103897.

Bai, J., Li, Y., Zhang, W., Liu, L., Wang, R., Qiu, Z., Liu, Y., Meng, Q., Zhang, Q., Yang, Z., Li, S., Wang, Y., Yue, S., 2023. Ammonia-oxidizing bacteria are the primary N_2O producers in long-time tillage and fertilization of dryland calcareous soil. Soil Tillage Res. 234, 105820. https://doi.org/10.1016/j.still.2023.105820.

Barth, G., VON Tucher, S., Schmidhalter, U., 2008. Effectiveness of 3,4-dimethylpyrazole phosphate as nitrification inhibitor in soil as influenced by inhibitor concentration, application form, and soil matric potenti. Pedosphere 18, 378–385.

Beeckman, F., Motte, H., Beeckman, T., 2018. Nitrification in agricultural soils: impact, actors and mitigation. Curr. Opin. Biotechnol. 50, 166–173. https://doi.org/10.1016/j.copbio.2018.01.014.

Bouwman, A.F., Boumans, L.J.M., Batjes, N.H., 2002. Modeling global annual N_2O and NO emissions from fertilized fields. Global Biogeochem. Cycles 16. https://doi.org/10.1029/2001gb001812.

Canadell, J.G., Monteiro, P.M.S., Costa, M.H., Cotrim da Cunha, L., Cox, P.M., Eliseev, A. V., Henson, S., Ishii, M., Jaccard, S., Koven, C., et al., 2021. Global carbon and other biogeochemical cycles and feedbacks. et al., eds.. In: Masson-Delmotte, V, Zhai, P,

Pirani, A, Connors, SL, Péan, C, Berger, S, et al. (Eds.), Climate Change 2021: The Physical Science Basis. Contribution of Working Group I to the Sixth Assessment Report of the Intergovernmental Panel On Climate Change. Cambridge University Press, Press, London, UK.

Caporaso, J.G., Kuczynski, J., Stombaugh, J., Bittinger, K., Bushman, F.D., Costello, E.K., Fierer, N., Peña, A.G., Goodrich, J.K., Gordon, J.I., Huttley, G.A., Kelley, S.T., Knights, D., Koenig, J.E., Ley, R.E., Lozupone, C.A., Mcdonald, D., Muegge, B.D., Pirrung, M., Reeder, J., Sevinsky, J.R., Turnbaugh, P.J., Walters, W.A., Widmann, J., Yatsunenko, T., Zaneveld, J., Knight, R., 2010. QIIME allows analysis of high-throughput community sequencing data. Nat. Methods 7, 335–336. https://doi.org/10.1038/nmeth0510-335.

Cui, X., Zhou, F., Ciais, P., Davidson, E.A., Tubiello, F.N., Niu, X., Ju, X., Canadell, J.G., Bouwman, A.F., Jackson, R.B., Mueller, N.D., Zheng, X., Kanter, D.R., Tian, H., Adalibieke, W., Bo, Y., Wang, Q., Zhan, X., Zhu, D., 2021. Global mapping of crop-specific emission factors highlights hotspots of nitrous oxide mitigation. Nat. Food 2, 886–893. https://doi.org/10.1038/s43016-021-00384-9.

De Boer, W., Kowalchuk, G.A., 2001. Nitrification in acid soils: micro-organisms and mechanisms. Soil Biol. Biochem. 33, 853–866. https://doi.org/10.1016/S0038-0717(00)00247-9.

Dong, D., Yang, W., Sun, H., Kong, S., Xu, H., 2021. Nitrous oxide emissions in response to long-term application of the nitrification inhibitor DMPP in an acidic luvisol. Appl. Soil Ecol. 159. https://doi.org/10.1016/j.apsoil.2020.103861.

Edgar, R.C., 2013. UPARSE: highly accurate OTU sequences from microbial amplicon reads. Nat. Methods 10, 996–998. https://doi.org/10.1038/nmeth.2604.

Fan, D., He, W., Smith, W.N., Drury, C.F., Jiang, R., Grant, B.B., Shi, Y., Song, D., Chen, Y., Wang, X., He, P., Zou, G., Chen, Y., Wang, X., He, P., Zou, G., 2022. Global evaluation of inhibitor impacts on ammonia and nitrous oxide emissions from agricultural soils: a meta-analysis. Glob. Chang. Biol. 28, 5121–5141. https://doi.org/10.1111/gcb.16294.

Fan, X., Yin, C., Chen, H., Ye, M., Zhao, Y., Li, T., Wakelin, S.A., Liang, Y., 2019. The eficacy of 3,4-dimethylpyrazole phosphate on N_2O emissions is linked to niche differentiation of ammonia oxidizing archaea and bacteria across four arable soils. Soil Biol. Biochem. 130, 82–93. https://doi.org/10.1016/j.soilbio.2018.11.027.

Fisk, L.M., Maccarone, L.D., Barton, L., Murphy, D.V., 2015. Nitrapyrin decreased ntrification of nitrogen released from soil organic matter but not amoA gene abundance at high soil temperature. Soil Biol. Biochem. 88, 214–223. https://doi.org/10.1016/j.soilbio.2015.05.029.

Friedl, J., Scheer, C., Rowlings, D.W., Deltedesco, E., Gorfer, M., Rosa, D.D., Grace, P.R., Müller, C., Keiblinger, K.M., 2020. Effect of the nitrification inhibitor (DMPP) on N-turnover, the N_2O reductase-gene *nos*Z and N_2O:N_2 partitioning from agricultural soil. Sci. Rep. 10, 2399. https://doi.org/10.1038/s41598-020-59249-z.

Hergoualc'h, K., Akiyama, H., Bernoux, M., Chirinda, N., del Prado, A., Kasimir, A., McDonald, J.D., Ogle, S.M., Regina, K., van der Weerden, T.J., 2019. N_2O emissions from managed soils, and CO_2 emissions from lime and urea application. 2019 Refinement to 2006 IPCC Guidel. Natl. Greenh. Gas Invent. 1–48.

Hernandez, D.J., David, A.S., Menges, E.S., Searcy, C.A., Afkhami, M.E., 2021. Environmental stress destabilizes microbial networks. ISME J. 15, 1722–1734. https://doi.org/10.1038/s41396-020-00882-x.

Herren, C.M., McMahon, K.D., 2017. Cohesion: a method for quantifying the connectivity of microbial communities. ISME J. 11, 2426–2438. https://doi.org/10.1038/ismej.2017.91.

Hink, L., Nicol, G.W., Prosser, J.I., 2017. Archaea produce lower yields of N_2O than bacteria during aerobic ammonia oxidation in soil. Environ. Microbiol. 19, 4829–4837. https://doi.org/10.1111/1462-2920.13282.

Jiang, L., Yu, J., Wang, S., Wang, X., Schwark, L., Zhu, G., 2023. Complete ammonia oxidization in agricultural soils: high ammonia fertilizer loss but low N_2O production. Glob. Chang. Biol. 29, 1984–1997. https://doi.org/10.1111/gcb.16586.

Kroon, P.S., Hensen, A., Van Den Bulk, W.C.M., Jongejan, P.A.C., Vermeulen, A.T., 2008. The importance of reducing the systematic error due to non-linearity in N_2O flux measurements by static chambers. Nutr. Cycl. Agroecosyst. 82, 175–186. https://doi.org/10.1007/s10705-008-9179-x.

Kumar, S., Stecher, G., Li, M., Knyaz, C., Tamura, K., 2018. MEGA X: molecular evolutionary genetics analysis across computing platforms. Mol. Biol. Evol. 35, 1547–1549. https://doi.org/10.1093/molbev/msy096.

Kurenbach, B., Marjoshi, D., Amábile-Cuevas, C.F., Ferguson, G.C., Godsoe, W., Gibson, P., Heinemann, J.A., 2015. Sublethal exposure to commercial formulations of the herbicides dicamba, 2,4-dichlorophenoxyacetic acid, and glyphosate cause changes in antibiotic susceptibility in Escherichia coli and Salmonella enterica serovar typhimurium. MBio 6, e00009–e00015. https://doi.org/10.1128/mBio.00009-15.

Lehtovirta-Morley, L.E., Ross, J., Hink, L., Weber, E.B., Gubry-Rangin, C., Thion, C., Prosser, J.I., Nicol, G.W., 2016. Isolation of "*Candidatus Nitrosocosmicus franklandus*", a novel ureolytic soil archaeal ammonia oxidiser with tolerance to high ammonia concentration. FEMS Microbiol. Ecol. 92, fiw057. https://doi.org/10.1093/femsec/fiw057.

Lei, J., Fan, Q., Yu, J., Ma, Y., Yin, J., Liu, R., 2022. A meta-analysis to examine whether nitrification inhibitors work through selectively inhibiting ammonia-oxidizing bacteria. Front. Microbiol. 13, 962146. https://doi.org/10.3389/fmicb.2022.962146.

Li, Z., Xu, P., Bo, X., Wu, J., Han, Z., Guo, S., Li, K., Shen, M., Wang, J., Zou, J., 2024. Soil pH-dependent efficacy of DMPP in mitigating nitrous oxide under different land uses. Geoderma 449, 117018. https://doi.org/10.1016/j.geoderma.2024.117018.

Li, Z., Xu, P., Han, Z., Wu, J., Bo, X., Wang, J., Zou, J., 2022. Effect of biochar and DMPP application alone or in combination on nitrous oxide emissions differed by soil types. Biol. Fertil. Soils 59, 123–138. https://doi.org/10.1007/s00374-022-01688-z.

Lin, Y., Ding, W., Liu, D., He, T., Yoo, G., Yuan, J., Chen, Z., Fan, J., 2017. Wheat straw-derived biochar amendment stimulated N_2O emissions from rice paddy soils by regulating the amoA genes of ammonia-oxidizing bacteria. Soil Biol. Biochem. 113, 89–98. https://doi.org/10.1016/j.soilbio.2017.06.001.

Liu, Q., Liu, B., Zhang, Y., Hu, T., Lin, Z., Liu, G., Wang, X., Ma, J., Wang, H., Jin, H., Ambus, P., Amonette, J.E., Xie, Z., 2019. Biochar application as a tool to decrease soil nitrogen losses (NH_3 volatilization, N_2O emissions, and N leaching) from croplands: options and mitigation strength in a global perspective. Glob. Chang. Biol. 25, 2077–2093. https://doi.org/10.1111/gcb.14613.

Nair, D., Abalos, D., Philippot, L., Bru, D., Mateo-Marín, N., Petersen, S.O., 2021. Soil and temperature effects on nitrification and denitrification modified N_2O mitigation by 3,4-dimethylpyrazole phosphate. Soil Biol. Biochem. 157, 108224. https://doi.org/10.1016/j.soilbio.2021.108224.

Nicol, G.W., Leininger, S., Schleper, C., Prosser, J.I., 2008. The influence of soil pH on the diversity, abundance and transcriptional activity of ammonia oxidizing archaea and bacteria. Environ. Microbiol. 10, 2966–2978. https://doi.org/10.1111/j.1462-2920.2008.01701.x.

Prasad, A.M., Iverson, L.R., Liaw, A., 2006. Newer classification and regression tree techniques: bagging and random forests for ecological prediction. Ecosystems 9, 181–199. https://doi.org/10.1007/s10021-005-0054-1.

Prosser, J.I., Hink, L., Gubry-Rangin, C., Nicol, G.W., 2020. Nitrous oxide production by ammonia oxidizers: physiological diversity, niche differentiation and potential mitigation strategies. Glob. Chang. Biol. 26, 103–118. https://doi.org/10.1111/gcb.14877.

Prosser, J.I., Nicol, G.W., 2012. Archaeal and bacterial ammonia-oxidisers in soil: the quest for niche specialisation and differentiation. Trends Microbiol. 20, 523–531. https://doi.org/10.1016/j.tim.2012.08.001.

R Core Team. 2021. R: a language and environment for statistical computing.

Ravishankara, A.R., Daniel, J.S., Portmann, R.W., 2009. Nitrous oxide (N_2O): the dominant ozone-depleting substance emitted in the 21st century. Science (80-) 326, 123–125. https://doi.org/10.1126/science.1176985.

Smith, M.S., Tiedje, J.M., 1979. Phases of denitrification following oxygen depletion in soil. Soil Biol. Biochem. 11, 261–267. https://doi.org/10.1016/0038-0717(79)90071-3.

Stieglmeier, M., Mooshammer, M., Kitzler, B., Wanek, W., Zechmeister-Boltenstern, S., Richter, A., Schleper, C., 2014. Aerobic nitrous oxide production through N-nitrosating hybrid formation in ammonia-oxidizing archaea. ISME J. 8, 1135–1146. https://doi.org/10.1038/ismej.2013.220.

Taylor, A.E., Taylor, K., Tennigkeit, B., Palatinszky, M., Stieglmeier, M., Myrold, D.D., Schleper, C., Wagner, M., Bottomley, P.J., 2015. Inhibitory effects of C_2 to C_{10} 1-alkynes on ammonia oxidation in two Nitrososphaera species. Appl. Environ. Microbiol. 81, 1942–1948. https://doi.org/10.1128/AEM.03688-14.

Tian, H., Xu, R., Canadell, J.G., Thompson, R.L., Winiwarter, W., Suntharalingam, P., Davidson, E.A., Ciais, P., Jackson, R.B., Janssens-Maenhout, G., Prather, M.J., Regnier, P., Pan, N., Pan, S., Peters, G.P., Shi, H., Tubiello, F.N., Zaehle, S., Zhou, F., Arneth, A., Battaglia, G., Berthet, S., Bopp, L., Bouwman, A.F., Buitenhuis, E.T., Chang, J., Chipperfield, M.P., Dangal, S.R.S., Dlugokencky, E., Elkins, J.W., Eyre, B. D., Fu, B., Hall, B., Ito, A., Joos, F., Krummel, P.B., Landolfi, A., Laruelle, G.G., Lauerwald, R., Li, W., Lienert, S., Maavara, T., MacLeod, M., Millet, D.B., Olin, S., Patra, P.K., Prinn, R.G., Raymond, P.A., Ruiz, D.J., van der Werf, G.R., Vuichard, N., Wang, J., Weiss, R.F., Wells, K.C., Wilson, C., Yang, J., Yao, Y., 2020. A comprehensive quantification of global nitrous oxide sources and sinks. Nature 586, 248–256. https://doi.org/10.1038/s41586-020-2780-0.

Tufail, M.A., Naeem, A., Arif, M.S., Farooq, T.H., Shahzad, S.M., Dar, A.A., Albasher, G., Shakoor, A., 2022. Unraveling the efficacy of nitrification inhibitors (DCD and DMPP) in reducing nitrogen gases emissions across agroecosystems: a three-decade global data synthesis (1993–2021). Fuel 324, 124725. https://doi.org/10.1016/j.fuel.2022.124725.

Vilarrasa-nogué, M., Teira-esmatges, M.R., Pascual, M., Villar, J.M., Rufat, J., 2020. Effect of N dose , fertilisation duration and application of a nitrification inhibitor on GHG emissions from a peach orchar. Sci. Total Environ. 699, 134042. https://doi.org/10.1016/j.scitotenv.2019.134042.

Wang, J., Smith, P., Hergoualc'h, K., Zou, J., 2022. Direct N_2O emissions from global tea plantations and mitigation potential by climate-smart practices. Resour. Conserv. Recycl. 185, 106501. https://doi.org/10.1016/j.resconrec.2022.106501.

Xu, S., Yu, Y., Fan, H., Bilyera, N., Meng, X., Xue, J., Lu, Z., Yang, Z., Chapman, S.J., Gao, F., Han, W., Li, Y., Zheng, N., Yao, H., Kuzyakov, Y., 2024. Microbial communities overwhelm environmental controls in explaining nitrous oxide emission in acidic soils. Soil Biol. Biochem. 194, 109453. https://doi.org/10.1016/j.soilbio.2024.109453.

Yamamoto, A., Akiyama, H., Naokawa, T., Miyazaki, Y., Honda, Y., Sano, Y., Nakajima, Y., Yagi, K., 2014. Lime-nitrogen application affects nitrification, denitrification, and N_2O emission in an acidic tea soil. Biol. Fertil. Soils 50, 53–62. https://doi.org/10.1007/s00374-013-0830-6.

Zerulla, W., Barth, T., Dressel, J., Erhardt, K., Horchler von Locquenghien, K., Pasda, G., Rädle, M., Wissemeier, A., 2001. 3,4-Dimethylpyrazole phosphate (DMPP) - a new nitrification inhibitor for agriculture and horticulture. An introduction. Biol. Fertil. Soils 34, 79–84. https://doi.org/10.1007/s003740100380.

Zhong, W., Bian, B., Gao, N., Min, J., Shi, W., Lin, X., Shen, W., 2016. Nitrogen fertilization induced changes in ammonia oxidation are attributable mostly to bacteria rather than archaea in greenhouse-based high N input vegetable soil. Soil Biol. Biochem. 93, 150–159. https://doi.org/10.1016/j.soilbio.2015.11.003.

Zou, J., Huang, Y., Jiang, J., Zheng, X., Sass, R.L., 2005. A 3-year field measurement of methane and nitrous oxide emissions from rice paddies in China: effects of water regime, crop residue, and fertilizer application. Global Biogeochem. Cycles 19, 1–9. https://doi.org/10.1029/2004GB002401.